Electronic structure of CuCl

Alex Zunger* and Marvin L. Cohen
Department of Physics, University of California, Berkeley, California 94720
and Materials and Molecular Research Division, Lawrence Berkeley Laboratory, Berkeley, California 94720

(Received 11 August 1978)

The electronic band structure of zinc-blende CuCl is computed using a self-consistent, first-principles, all-electron approach. The calculated energy levels agree with photoemission results and support a minimum-direct-gap interpretation of the optical data. Contrary to the indirect model proposed by Rusakov and used by Abrikosov to explain superdiamagnetism and/or high-temperature superconductivity, the calculated band-pressure coefficients do not yield an indirect gap at the pressure where anomalies appear.

Recent experimental measurements[1-3] of anomalously large diamagnetism in CuCl have stirred considerable interest in the possibility of high-temperature ($\sim 150°$ K) superconductivity in this material. Abrikosov[4] has proposed an electron-hole mechanism for high-temperature superconductivity and has applied this theory to CuCl based on a model of the electronic structure of CuCl which was proposed by Rusakov *et al.*[5,6] The essential feature of the Rusakov model is an indirect band gap for CuCl, small enough to be comparable to an exciton binding energy (~ 0.3 eV). The model assumes that under pressure the conduction-band edge, which is at $\vec{k} \neq 0$, will move to lower energies and form an "excitonic dielectric"[1,4] with small-mass electrons at $\vec{k} \neq 0$ and heavy-mass holes at $\vec{k} = 0$. Rusakov *et al.*[5,6] suggest that the conduction-band minimum is in the [100] direction near X and have interpreted optical data based on this model. The Abrikosov explanation of high-temperature superconductivity in CuCl rests on this model.

Although the phase diagram of CuCl shows a large number of structures in a relatively narrow parameter range (e.g., Ref. 5 and references therein), the reported Meissner-like effect was observed at pressures as low as 5 kbar,[5] below the first isostructural transition.[5] It hence seems important to assess whether the band structure of the ideal zinc-blende structure (i.e., the observed low-pressure form), as well as that of its isostructurally compressed forms lends support to the model put forward by Rusakov *et al.*

Although previous band calculations on CuCl exist in the literature,[7-9] the use of empirical spectral data (which does not appear to support Rusakov's model) to fit the bands,[7,8] the introduction of spherical approximations to the crystal potential,[9] and the lack of any self-consistency[7-9] might have introduced an unwarranted bias in the results. To test the indirect gap model and hence the Abrikosov suggestion we have used a self-consistent, nonempirical all-electron approach[10] to compute the electron structure of ideal CuCl. Contrary to the suggestion of Rusakov,[5,6] Brandt *et al.*,[1] and Abrikosov[4] we find that ideal zinc-blende CuCl has a minimum direct gap at Γ. The calculated pressure coefficients for the ground state also indicate that band edges at $\vec{k} \neq 0$ will not become the conduction-band minimum for the pressure range considered in the experiments by Brandt *et al.*,[1] and Chu *et al.*[2]

The calculational method has been previously described[10] and applied to a wide range of insulating, metallic, and semiconducting compounds (Ref. 11 and references therein). In the present application the crystal wave function $\psi_j(\vec{k}, \vec{r})$ are expanded in a Bloch basis constructed from accurate (numerical) eigenstates $\chi_{nl}(r, \{f_{nl}^{\alpha} Q^{\alpha}\})$ of the isolated Cu^{Q+} and Cl^{Q-} species (with fractional charge Q) where f_{nl}^{α} denotes the (possibly noninteger) occupation numbers of Cu $1s, 2s, 3s, 3p, 3d, 4s, 4p$ and Cl $1s, 2s, 2p, 3s, 3p$. Additional Slater-type Cl $3d$ and $4s$ orbitals are added for greater variational flexibility (addition of further Cu s orbitals affected the band gap by less than 0.1 eV). As the particular choice of basis orbitals which corresponds to the *ground-atomic* state (i.e., charges of $Q^{Cu} = Q^{Cl} = 0$ and $f_{3d}^{Cu} = 10$, $f_{4s}^{Cu} = 1$, $f_{4p}^{Cu} = 0$, and $f_{3s}^{Cl} = 2$, $f_{3p}^{Cl} = 5$) is not necessarily effective in expanding $\psi_j(\vec{k}, \vec{r})$ for a partially ionic solid such as CuCl, we have introduced the orbital charge-redistribution effects in the *basis set* by explicitly optimizing $\{f_{nl}^{\alpha}, Q^{\alpha}\}$. This is done by selecting from all ground and excited sets $\chi_{nl}(r, \{f_{nl}^{\alpha}, Q^{\alpha}\})$ of the Cu^{Q} and Cl^{Q-} species the one that leads to a minimization over the unit cell space of the difference $\Delta\rho(\vec{r})$ between the variational *crystal* charge density $\rho_{cry}(\vec{r})$ [obtained by solving the crystal Hamiltonian for $\psi_j(\vec{k}, \vec{r})$ at the $\vec{k} = \Gamma$, X, L, W, Σ, and Δ points in the zone, using a Bloch representation for $\chi_{nl}(r, \{f_{nl}^{\alpha}, Q^{\alpha}\})$] and the *superposition* charge density

$\rho_{\text{sup}}(\vec{r}) = \sum_{p,\alpha} \chi^2_{nl}(\vec{r} - \vec{R}_p - \vec{\tau}_\alpha)$. Here $\vec{R}_p$ and $\vec{\tau}_\alpha$ denote the translationally equivalent and inequivalent position vectors, respectively. This charge-and-configuration self-consistency (CCSC) yields the effective configuration of the ions in the crystal, which describes best (in the least-mean-square sense) the variational density $\rho_{\text{cry}}(\vec{r})$ in terms of a superposition of overlapping ionic charge densities. Since the residual density $\Delta\rho(\vec{r})$ (which is not describable in terms of densities of superposed ions) is non-negligible, we go in the second stage of the calculation beyond the CCSC to "full" self-consistency by directly incorporating the minimized (anisotropic) $\Delta\rho(\vec{r})$ in the crystal potential $V[\rho_{\text{sup}} + \Delta\rho]$ using reciprocal-space iterative techniques.[10] The effects introduced thereby are significant on the energy scale pertinent to the suggested band models[5-6] for CuCl (i.e., the band gap increases by about 0.7 eV relative to the optimized superposition model). It is nevertheless instructive to consider the nature of the effective ionic configuration in the solid at the CCSC stage. We obtain $Cu^{0.40+}\ 3d^{9.53}4s^{0.67}4p^{0.40}$ and $Cl^{0.40-}\ 3s^{1.98}3p^{5.42}$ (the occupations of the lower-lying orbitals being essentially unchanged from the ground state), indicating a reduction in the Cu-$3d$ occupation relative to the atomic $3d^{10}$ ground state (at the expense of shifting some Cu-d character into other bands), a covalent s to p promotion on Cu and an overall ionic Cu to Cl charge transfer of $0.4e$. The occurance of an effective Cu-$3d^{9.5}$ configuration, midway between the divalent $3d^9$ and the monovalent $3d^{10}$ forms, is suggestive of the tendency of CuCl to disproportionate into $CuCl_2$.[12] We find that a simple superposition-model calculation with a $3d^{10}$ configuration yields a metallic system, while a decrease in the Cu-d population tends to open up the gap (e.g., a gap of 0.6 eV is found for Cu $3d^{9.8}$). This behavior parallels the situation in the isolated $Cu^{Q+}\ 3d^{10-Q}$ system where increasing Q from zero increases significantly the s-d separation due to the relative stabilization of the $3d$ state via a partial relief of the strong intrasite Coulomb repulsion.[13] It also dramatizes the need for an accurate self-consistent treatment which avoids a bias in determining the effective electronic configuration in the solid. In the present calculation the crystal potential $V(\rho(\vec{r}))$ is constructed from all core+valence Coulomb contributions as well as from the respective local-density functional (LDF) exchange (with coefficient $\alpha = \frac{2}{3}$) and correlation potentials.[14] All interactions within a radius of 25 a.u. are included, and spherical approximations are avoided.

The self-consistent band structure of CuCl for the equilibrium lattice parameter $a = 10.215$ a.u. is shown in Fig. 1. Figure 2 depicts the energy variation of some of the band states at high-symmetry points with the lattice parameter $a = a_0 + \Delta a$ where $\Delta a = -0.6$, -0.4, -0.2, and 0.2 a.u.

CuCl appears to be a simple direct-gap insulator

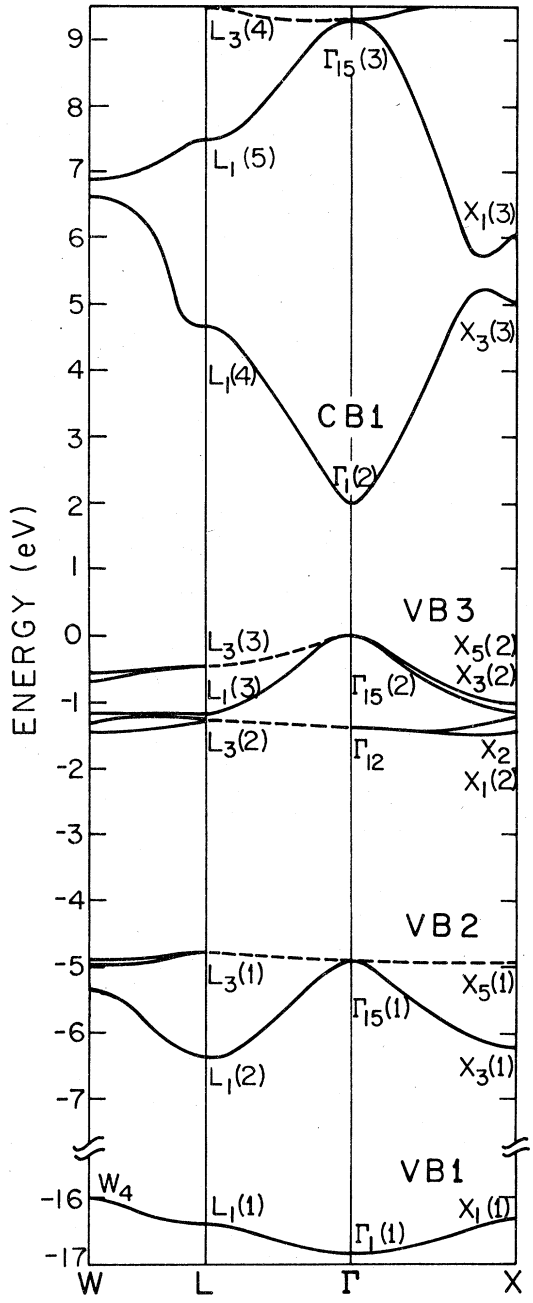

FIG. 1. Self-consistent exchange and correlation band structure of cubic CuCl at the low-pressure lattice parameter. Broken lines indicate double degenerate representations. The labels in parenthesis denote the order of the representations. 24 $\vec{k}$ points were used.

with no evidence for an indirect gap at L or X at any of the unit-cell volumes studied. This agrees with the conclusions of Khan[15] and Calabrese and Fowler,[7] based on empirical model calculations. The valence bands split into three major nonoverlapping bands (VB1 to VB3, c.f. Fig. 1): the lowest VB1 band is

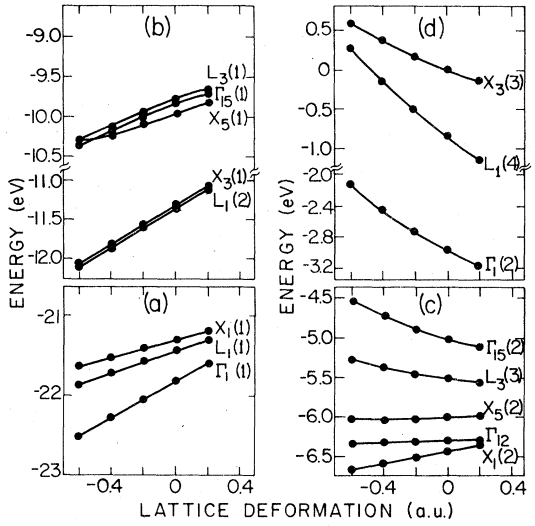

FIG. 2. Variation of the band states at high-symmetry points in the zone with the lattice parameter shift Δa. Full dots indicate calculated points. (a) VB1, (b) VB2, (c) VB3, (d) CB1.

predominantly (90%) of Cl-3s character, has a small (0.5 eV) width and is separated by 10 eV (at L) to 12 eV (at Γ) from the Cl-3p-derived (75%) band VB2. The two Cl-based bands VB1 and VB2 are separated by a 3.5-eV gap from the main Cu-3d-based VB3 band. The latter has a nearly dispersionless subband $L_3(2)$ - Γ_{12} - $X_1(2)$ and a wider (1.5 eV) subband at higher energies which contain 24% of Cl-3p and 76% Cu-3d character at the zone center. This gives rise to a two-peak structure in the VB3 density of states with a 0.95 eV separation. The magnitude of these orbital hybridizations (determined here from the Mulliken population analysis of the bands) agrees well with the experimentally deduced values based on exciton spin-orbit splitting[8] (25% Cl 3p), exciton g factor[16] ($23 \pm 2\%$ Cl 3p) and x-ray[17] and uv[8] photoelectron spectra (24% Cl 3p). At the zone center the lowest conduction band (CB1, with an electron effective mass of 0.42 m_e) is composed of Cu 4s (with some Cl-3s admixture), with increasing proportions of Cu 4p and Cl 3d towards the zone boundaries [e.g., 25% at $L_1(4)$].

We find that the charge density at $\Gamma_1(2)$ has a large amplitude *on the* Cl *site,* due to the enhanced range of the somewhat depopulated Cu 4s orbital. This suggests that the polarity of the crystal upon excitation into the lowest conduction band (or into the excitons converging to it) would be substantially larger than in the ground state. Because of this strong excited-state polarization, electrons may couple to the polarization field more strongly than in the ground state.

Note that the principal VB3-CB1 band gap E_g is largely *homopolar,* separating a predominantly Cu 3d from a Cu 4s state (a small ionic contribution is associated with the admixture of Cl character into VB3). This makes E_g (calculated value: 2 eV) extremely sensitive to the s (d) population of Cu. The VB2-CB1 gap on the other hand is largely heteropolar, much like the principle gap in nontransition-metal tetrahedrally bonded semiconductors and ionic solids. We conclude that two distinct mechanisms are responsible for the formation of a large direct gap in CuCl: (i) the intrasite (homopolar) d to sp charge promotion which opens up the s-d gap, much like evidenced in the isolated Cu^{Q+} system for $Q > 0$. This contribution to the gap can be obtained already at the level of a superposition-model calculation with a properly selected electronic configuration. (ii) the further opening of the gap due to the intersite (heteropolar) hybridization effects introducing an ionic component which scales like the charge transfer. This contribution is accurately obtained only in a self-consistent calculation which does not constrain the crystal charge density to a cellular representation (e.g., muffin-tin or superposition models).

Table I compares the calculated interband transition energies with the optical data.[8,18,19] These are grouped into VB3→CB1 transitions (transitions 1-6), VB2→CB1 transitions (7-12), and VB1→CB1 (13-15) where the first two groups overlap strongly. The agreement with experiment is generally very good except for the value of the gap which is too low by 40%. This is a general feature of the density functional approach where gaps coupling a localized with a delocalized state are usually *underestimated* by as much as 20%–40%. It results from two competing effects: whereas the introduction of orbital relaxation *reduces* the one-electron band structure prediction of the gap, the removal of the electron self-interaction akin to the LDF tends to *increase* it. Simple atomic *total energy* difference calculations in the LDF for Cu $3d^n4s^m \rightarrow 3d^{n-1}4s^{m+1}$ ($9 \leq n \leq 10$; $0 \leq m \leq 1$) indicate that the net effect is to *increase* the one-electron prediction for the d-s gap by 1.0–1.5 eV. This atomic estimate forms an upper bound as the crystal screening would tend to reduce this correction. However, due to the insulating characteristics of the screening in CuCl and the occurence of a relatively narrow d band, one expects that these corrections to the band-structure gap would not change significantly from the simple atomic estimate. Both long-range (polaron type) correlations and the intrasite Coulomb repulsions (Hubbard type) are expected to further modify the gap. Transitions at higher energies, not involving the localized VB3 states (c.f. Table I), are in better agreement with experiment due to the decreasing role of relaxation and self-interaction effects.

We emphasize here that the relaxation of self-interaction-compensation corrections to the one-electron gap occur both for a choice of small exchange coefficient ($\alpha = \frac{2}{3}$) as well as for a larger exchange parameter ($\alpha = 1$) and that they persist over a

TABLE I. Calculated and observed interband transition energies in CuCl. The experimental notation is given in parenthesis. Results are given in eV.

States	Calc. Energy	Experimental
1) $\Gamma_{15}(2) \rightarrow \Gamma_1(2)$	2.0	3.4[a,b]
2) $X_5(2) \rightarrow X_3(3)$	6.1	6.3[a] (E_1)
2) $L_3(3) \rightarrow L_1(4)$	5.7	6.3[a] (E_1)
3) $X_5(2) \rightarrow X_1(3)$	7.0	6.8,[a] 6.5[b] (E_0')
4) $L_3(3) \rightarrow L_1(5)$	8.0	8.3,[a] 8.3[b] (E_{2A})
5) $L_3(3) \rightarrow L_3(4)$	9.9	10,[a] 9.9[b] (E_{2B})
6) $X_1(2),\ X_2 \rightarrow X_5(3)$	13.9	14.2[c]
7) $\Gamma_{15}(1) \rightarrow \Gamma_1(2)$	6.8	6.8,[a], 6.5[b] (E_0')
8) $X_5(1) \rightarrow X_3(3)$	10.0	10,[a] 9.9[b] (E_{2B})
9) $L_1(2) \rightarrow L_1(4)$	11.1	11.9[c]
10) $L_3(1) \rightarrow L_1(5)$	11.9	
11) $L_1(2) \rightarrow L_3(4)$	15.9	16.0[c]
12) $X_5(1) \rightarrow X_5(3)$	17.5	17.5[c]
13) $\Gamma_1(1) \rightarrow \Gamma_1(2)$	18.8	
14) $L_1(1) \rightarrow L_1(4)$	21.2	19-21[c]
15) $X_1(1) \rightarrow X_3(3)$	21.3	

[a]Reference 8. [b]Reference 18. [c]Reference 19.

large range of assumed electronic populations n and m. Hence, although a one-electron band structure with $\alpha = 1$ or with an assumed non-self-consistent atomic configuration of Cu $3d^9$ produces in CuCl a large gap (3.2 and 3.4 eV, respectively, with the present method) due to the stabilization of the localized VB3 band with respect to the more diffused CB1 band, the agreement with the experimental gap (3.4 eV) might be fortuitous. The consistent choice of a Kohn and Sham exchange ($\alpha = \frac{2}{3}$) plus the homogeneous correlation term[14] used here yields in turn a smaller one-electron gap (2.0 eV) plus an estimated nonlocality correction of 1.0–1.5 eV.

Although more sophisticated estimates of these corrections are undoubtedly desirable (e.g., by a transition-state embedded cluster approach), we feel that even our simple estimate points to a dramatic breakdown of the simple band-structure model for CuCl.

Table II depicts the main predicted structures in the calculated density of states, as compared with uv[8] and x-ray[16] photoemission results. The agreement is seen to be very good. Note however that due to the extreme localization of the flat $L_3(2) - \Gamma_{12} - X_1(2)$ subband, the calculated one-electron separation between VB3 and VB2 might be considerably modi-

TABLE II. Comparison of calculated structure in the density of states with the observed photoemission data (in eV).

Structure	Assignment	Calc. Energy	Experimental
I	$L_3(3),\ X_5(2)$	0.9 ± 0.2	0.82,[a] 1.0[b]
II	$\Gamma_{12},\ L_3(2)$	1.4 ± 0.1	1.93,[a] 2.0[b]
III	$L_3(1) - \Gamma_{15}(1) - X_5(1)$	4.85 ± 0.1	4.87,[a] 5.1[b]
IV	$L_1(2) - X_3(1)$	6.3 ± 0.1	6.2,[a] 6.3[b]

[a]Reference 8. [b]References 16 and 17.

fied via strong orbital-relaxation effects.

Reduction of the lattice parameter causes a destabilization of the lower conduction bands CB1 [Fig. 2(d)] with a deformation potential $D_j(\vec{k}) = \partial E_j(\vec{k})/\partial \ln \Omega$ of $-(3-5)$ eV whereas the upper valence bands VB3 [Fig. 2(c)] have a somewhat lower deformation potential of $-(2 \pm 1)$ eV. This leads to a negative $\Delta D_{ij}(\vec{k})$ for the direct gap at Γ ($\Delta D = -2.3$ eV) and the indirect $\Gamma - X$ gap, in contrast with the suggestion of Rusakov.[20] Note however, that as an electron *excited* into the $\Gamma_1(2)$ level has most of its density near the Cl site, the attractive point-ion electrostatic field on the Cl sublattice would tend to lower this band with pressure, partially reducing the repulsive-pressure effect evident from the present calculation for the *unoccupied* CB1 state [Fig. 2(d)]. The observed deformation potential of the exciton transitions[21] is only slightly negative ($\Delta D = -0.4$ eV). We note in passing that the deformation potential changes sign in moving downwards from the upper edge of VB3. Experimental studies of such effects would seem important in assessing the validity of the present calculation.

On the basis of our result, the Rusakov model for the band structure of CuCl appears unlikely, and therefore the application of the Abrikosov mechanism to zinc-blende CuCl is inappropriate. Hence, if the experimental measurements on anomalous diamagnetism in CuCl are valid, other explanations are necessary.

This work was supported in part by the Division of Basic Energy Sciences, U.S. DOE and by NSF Grant No. DMR76-20647-AO1. One of us (A.Z.) received support from IBM.

---

*Present address. Solar Energy Res. Inst., Photovoltaics Branch, Golden, Colo. 80401

[1]N. B. Brandt, S. V. Kuvshinnikov, A. P. Rusakov, and M. V. Semenov, Pis'ma Zh. Eksp. Teor. Fiz. JETP 27, 37 (1978) [JETP Lett. 27, (1978)].

[2]C. W. Chu, A. P. Rusakov, S. Huang, S. Early, T. Geballe, and C. Y. Huang (unpublished).

[3]I. Lefkowitz, P. Bloomfield, and J. Manning (unpublished).

[4]A. A. Abrikosov, Pis'ma Zh. Eksp. Teor. Fiz. JETP 27, 235 (1978) [JETP Lett. 27, (1978)].

[5]A. P. Rusakov, N. V. Fistul', M. A. Il'in, A. A. Abdulaev, and S. G. Grigoryan, Sov. Phys. Solid State 18, 2067 (1976).

[6]A. P. Rusakov, Phys. Status Solidi B 72, 503 (1975).

[7]E. Calabrese and W. B. Fowler, Phys. Status Solidi B 57, 135 (1973).

[8]A. Goldman, J. Tejeda, N. J. Schevchik, and M. Cardona, Phys. Rev. B 10, 4388 (1974); M. Cardona, Phys. Rev. 129, 69 (1963).

[9]K. S. Song, J. Phys. Chem. Solids 28, 2003 (1967).

[10]A. Zunger and A. J. Freeman, Phys. Rev. B 15, 4716 (1977).

[11]E. G. see A. Zunger and A. J. Freeman, Phys. Rev. B 15, 5049 (1977); B 16, 906 (1977); B 16, 2901 (1977); and B 17, 2030 (1977); and Phys. Rev. Lett. 40, 1155 (1978).

[12]Similar calculation on the fictitious zinc-blende CuF yields an effective Cu-$3d^{9.1}$ configuration suggesting that the divalent CuF_2 ($3d^9$) is more stable.

[13]Calculated (LDF) atomic *s-d* splitting increases from 0.5 eV at the $3d^{10}4s^1$ configuration to 4–5 eV (depending on the exchange approximation) at the $3d^94s^2$ configuration. Hence band calculations using incomplete self-consistency and near-$3d^{10}$ configurations show artificially small gaps.

[14]K. S. Singwi, A. Sjölander, P. M. Tosi, and R. H. Land, Phys. Rev. B 1, 1044 (1970).

[15]M. A. Khan, Solid State Commun. 11, 587 (1972).

[16]S. Suga, T. Koda, and T. Mitani, Phys. Status Solidi B 48, 753 (1971).

[17]S. Kono, T. Ishii, T. Sagawa, and T. Kobayashi, Phys. Rev. Lett. 28, 1385 (1972); Phys. Rev. B 8, 795 (1973).

[18]H. Fesefeldt, Z. Phys. 67, 37 (1931); E. G. Schneider and H. M. O'Brayn, Phys. Rev. 51, 293 (1973).

[19]S. Sato, T. Ishii, I. Nagakura, O. Aita, S. Ankai, M. Yokota, K. Ichikawa, G. Matsuoka, S. Kono, and T. Sagawa, J. Phys. Soc. Jpn. 30, 459 (1971).

[20]Note that the faster increase in the $\Gamma_1(2)$ energy, relative to $X_3(3)$, with reducing the unit-cell volume indeed causes a reduction in the $\Gamma_1(2) - X_3(3)$ splitting (of 0.4 eV in the studied volume range). However, this reduction is too small to cause a near degeneracy even when the energies of the respective states are corrected for relaxation and self-interaction.

[21]J. B. Anthony, A. D. Brothers, and D. W. Lynch, Phys. Rev. B 5, 3189 (1972).